IEEE Access
Multidisciplinary : Rapid Review : Open Access Journal

Received 15 February 2023, accepted 30 March 2023, date of publication 5 April 2023, date of current version 12 April 2023.

Digital Object Identifier 10.1109/ACCESS.2023.3264801

RESEARCH ARTICLE

Generation of Limit Cycles in Nonlinear Systems: Machine Leaning Based Type-3 Fuzzy Control

BICHENG YAN[1], XIAOQIANG JIANG[1], KHALID A. ALATTAS[2], CHUNWEI ZHANG[3], AND ARDASHIR MOHAMMADZADEH[3]

[1]Intelligent Manufacturing School, Zhejiang Institute of Mechanical & Electrical Engineering, Hangzhou 310059, China
[2]Department of Computer Science and Artificial Intelligence, College of Computer Science and Engineering, University of Jeddah, Jeddah 23890, Saudi Arabia
[3]Multidisciplinary Center for Infrastructure Engineering, Shenyang University of Technology, Shenyang 110870, China

Corresponding authors: Chunwei Zhang (zhangchunwei@sut.edu.cn) and Ardashir Mohammadzadeh (a.mzadeh@sut.edu.cn)

This work was supported in part by the Ministry of Science and Technology of China under Grant 2019YFE0112400, and in part by the Department of Science and Technology of Shandong Province under Grant 2021CXGC011204.

ABSTRACT A limit cycle is a cyclic path of oscillation on which the states of a nonlinear system settle. A considerable number of practical systems such as robots, converters, and heartbeat require generating the sustainable oscillatory behaviours. The objective is to design a controller to generate limit cycle with specific behaviours. In this paper, a novel fuzzy control (FC) strategy is introduced to create the limit-cycle for nonlinear complex dynamics with unknown uncertainties. The suggested controller benefits from new interval type-3 fuzzy logic, allowing the control synthesis to improve the quality of closed-loop response and robust performance. The adaptively learned backstepping controller based on FC is employed to analyze the convergence and robustness. Various simulations are proposed to ensure the efficiency of the fuzzy-based control law and adaption rules.

INDEX TERMS Fuzzy logic, type-3 fuzzy control, limit cycle, machine learning, control.

I. INTRODUCTION

For applications where the goal is to create oscillating motion, the limit cycle is a very useful characteristic. Finding a cycle is usually very difficult. LCs can be stable, unstable, or semi-stable. Semi-stable limit cycles are cycles that are stable for initial values inside the region enclosed by the limit cycle and unstable for other regions [1].

In general, generating limit cycle (LC) needs analysis of invariant sets rather than equilibrium points, thereby the Lyapunov concepts should be revised to handle the problem. In nonlinear systems, a nonlinear control law such as backstepping policy is required to be designed such that trajectories of a system converge to the desired LC. Moreover, generating stable oscillations based on LC controller may subject to external perturbations. Therefore, the robustness of a system needs to be investigated. In the literature, a few number of papers explored the self-sustained LC design procedure. For instance, a harmonic oscillator was designed for nonlinear systems based on a backstepping procedure in [2], resulting in generating appropriate self-sustained LC. Authors in [3] investigated the LC design for elastic joint robots for regulating of the proposed energy function for the system. The LC synthesis with tracking problem was studied for systems exposed to uncertainties and disturbances [4]. Authors in [5] designed a sliding mode controller for the LC with dead-zone nonlinearity. The design procedure was also developed for time-delay systems [6] using concept of positive limit sets. Moreover, synthesizing stable LC has been investigated for discrete-time dynamics and in versus disturbances [7], [8]. The LC control problem was studied by describing function method and reducing the changes in LC amplitude and frequency [9]. The generation of the LC with matched/unmatched uncertainties was analyzed in [10]. Resorting to a port-hamiltonian model-based controller by Hamiltonian function, the LC was designed in [11].

On the other hand, robust control techniques were used for the stabilization of systems with uncertainties. For example, super twisting sliding mode controller in [12] to deal with external disturbances, robust MPC [13] for bounded disturbances, robust MPC to tackle parametric uncertainties [14],

The associate editor coordinating the review of this manuscript and approving it for publication was Yu-Da Lin.

robust H_∞ control in [15], have all been suggested in the past couple of years.

Furthermore, the fuzzy logic systems have been suggested in the literature widely to analyze and identify complexities of the model for nonlinear systems. For instance, The concept of fuzzy control has been also developed by using fuzzy logic systems for systems without exact model and detailed information of uncertainties and disturbances [16], [17]. Note that there exists a significant number of papers in this field. For instance, fractional order fuzzy control [18], type-2 (T2) fuzzy with event-triggered mechanisms [19], non-singleton type 2 fuzzy [20], and fuzzy output feedback for strict systems [21] have been proposed. Moreover, a tracking problem of a mobile-robot was studied by a T2-FC as a torque control and genetic algorithms in [22]. A number of techniques were utilized to develop the fuzzy based controllers [23] in terms of reducing error signals. For tuning fuzzy logic systems, authors in [24] suggested Ant Colony optimization algorithms and then applied the fuzzy control to the mobile-robot system. The interval T2-FC was employed for a pH neutralization experimental setup in [25]. The suggested fuzzy logic system then extended based on optimization techniques such as bang-big optimization in [26]. Recently, interval type 3 fuzzy controllers have been employed for stabilization with unknown dynamics [27], [28]. This approach is able to increase the estimation accuracy, leading to robust performance against unknown uncertainties without any information of the upper bound or interval of variations [29], [30]. Based on type-3 fuzzy controls, uncertainties of systems with a wider range of variations and higher values can be analyzed [31], [32], [33].

Based on the literature review, the issue of LC synthesis of nonlinear systems with unknown uncertainties is of utmost importance and a fuzzy logic system can be used to tackle the problem, resulting in creating the appropriate LC for a wide range of physical plants with unknown uncertainties. The aim is that the trajectories converge to the desired LC and remaining in a boundary layer in the presence of uncertainties. First, the LC control is proposed for the considered second-order system, and then the stability of generated LC is analyzed by a Lyapunov approach. A novel interval fuzzy-based adaptive backstepping controller is also employed such that appropriate stable oscillations are generated in the general form. Since the system is exposed to unknown uncertainties, the FC is used to estimate them. It is noticeable that the advanced interval type 3 fuzzy-based control policy is responsible for the approximation of uncertain dynamics and disturbances, resulting in high accuracy and the rapid speed of the convergence of error signals to zero and simultaneously state trajectories to the limit cycle. As far as the authors know, this matter has not been fully address yet, and the design method of this paper outperform previous papers since they all required exact model information of the system. To conclude, the main contributions and difficulties are listed as bellow:

- The FC is designed based on error signals to ensure the robustness of a wide range of nonlinear systems exposed to external disturbances/uncertainties without having information about their variations. To construct the type 3 fuzzy logic systems, it is important to optimize the training parameters based on adaptive rules and devise membership functions in a way that the degree of freedom increases. Previous methods dealt with the LC generations did not benefit from type 3 FLS. Although improving the quality of approximation brings complexities in designing the FC, having more degree of freedom in the choice of parameters leads to better approximation ability and more flexibility in terms encountering model uncertainties. Therefore, the method of this paper is more useful in practice when the variations of uncertainties are high and impossible to predict or measure.
- The reference trajectories converges to the desired cyclic path in a fast time due to the adaptive mechanism employed in the structure of the control law.
- Lyapunov scheme is used to analyze the stability of trajectories required to converge to the cyclic path which in turn the robust stability is guaranteed in the under the uncertainties.

II. PROBLEM FORMULATION

$$\begin{aligned}
\dot{y}_1 &= y_2 \\
\dot{y}_2 &= f_2(y_1, y_2) + g_2(y_1, y_2)y_3 + F_2(y) \\
&\vdots \\
\dot{y}_n &= f_n(y) + g_n(y)\, y_3 + F_n(y) \; + u
\end{aligned} \tag{1}$$

where $y = [y_1, y_2, \ldots, y_n]^T$ is the state variable, $f(.)/g(.)$ are nonlinearities while $F(.)$ is an unknown function to be approximated and u denotes controller. The objective is to produce a LC in the existence of unknown an unknown function and with predefined amplitude and frequency (see Figs. 1- 2). As a result, the trajectories should converge to the prescribed LC with following property

$$L = \{y \in D \subseteq \mathbb{R}^n | \psi\,(y_1, y_2) = r^2\} \tag{2}$$

where $\psi\,(y_1, y_2)$ is a differentiable function and $r > 0$ is a positive constant.

Definition 1: $\dot{y} = f(y)\,(y \in D \subseteq \mathbb{R}^n)$ with $L \subseteq D$ is a closed invariant set, if there exists a $V(y)$ such that

- *$V(y) = 0$ on the set L.*
- *$V(y) > 0$ in some neighbourhood of L, excluding L.*
- *$\dot{V}(y) < 0$ in D, except L.*

Then, L is an exponentially stable positive LC.

III. TYPE-3 FUZZY CONTROL

In this section we illustrate the structure of type-3 fuzzy control as depicted in Fig. 3.

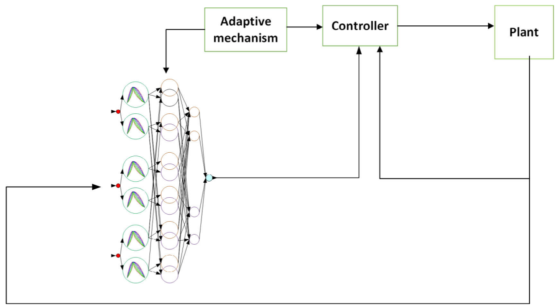

FIGURE 1. General diagram.

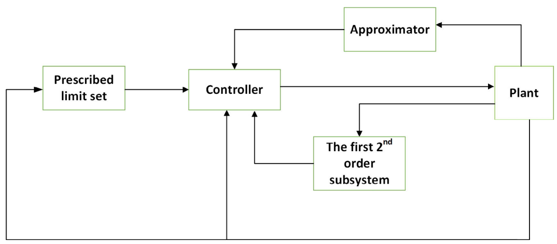

FIGURE 2. General diagram.

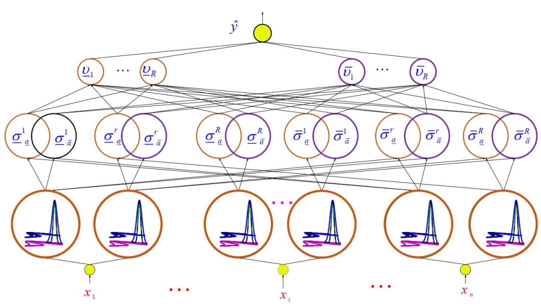

FIGURE 3. Structure of type-3 fuzzy control.

1) The inputs are $y_1(t), \ldots, y_n(t)$. 2) For all inputs, the upper/lower memberships are obtained as:

$$\bar{\sigma}_{m^j_{i,\bar{a}_k}}(y_i) = \exp\left(-\frac{\left(y_i - \chi_{m^j_{i,\bar{a}_k}}\right)^2}{\bar{\Xi}^2_{m^j_{i,\bar{a}_k}}}\right) \tag{3}$$

$$\bar{\sigma}_{m^j_{i,\underline{a}_k}}(y_i) = \exp\left(-\frac{\left(y_i - \chi_{m^j_{i,\underline{a}_k}}\right)^2}{\bar{\Xi}^2_{m^j_{i,\underline{a}_k}}}\right) \tag{4}$$

$$\underline{\sigma}_{m^j_{i,\bar{a}_k}}(y_i) = \exp\left(-\frac{\left(y_i - \chi_{m^j_{i,\bar{a}_k}}\right)^2}{\underline{\Xi}^2_{m^j_{i,\bar{a}_k}}}\right) \tag{5}$$

$$\underline{\sigma}_{m^j_{i,\underline{a}_k}}(y_i) = \exp\left(-\frac{\left(y_i - \chi_{m^j_{i,\underline{a}_k}}\right)^2}{\underline{\Xi}^2_{m^j_{i,\underline{a}_k}}}\right) \tag{6}$$

3) The $r-th$ rule is:

$$\text{Rule\#}r\text{: If } y_1 \text{ is } m^r_{1,\bar{a}_k} \text{ and } y_2 \text{ is } m^r_{2,\bar{a}_k} \text{ and } y_3 \text{ is } m^r_{3,\bar{a}_k} \text{ Then } \hat{y} \in \left[\underline{y}_r, \bar{y}_r\right] \tag{7}$$

where, $m^r_{1,\bar{a}_k}$, $m^r_{2,\bar{a}_k}$ and $m^r_{3,\bar{a}_k}$ are r-th MF for y_1, y_2 and y_3. The firings are:

$$\underline{\upsilon}^r_{\bar{a}_k} = \underline{\sigma}_{m^{j1}_{1,\bar{a}_k}}(y_1)\,\underline{\sigma}_{m^{j2}_{2,\bar{a}_k}}(y_2)\,\underline{\sigma}_{m^{j3}_{3,\bar{a}_k}}(y_3) \tag{8}$$

$$\underline{\upsilon}^r_{\underline{a}_k} = \underline{\sigma}_{m^{j1}_{1,\underline{a}_k}}(y_1)\,\underline{\sigma}_{m^{j2}_{2,\underline{a}_k}}(y_2)\,\underline{\sigma}_{m^{j3}_{3,\underline{a}_k}}(y_3) \tag{9}$$

$$\bar{\upsilon}^r_{\bar{a}_k} = \bar{\sigma}_{m^{j1}_{1,\bar{a}_k}}(y_1)\,\bar{\sigma}_{m^{j2}_{2,\bar{a}_k}}(y_2)\,\bar{\sigma}_{m^{j3}_{3,\bar{a}_k}}(y_3) \tag{10}$$

$$\bar{\upsilon}^r_{\underline{a}_k} = \bar{\sigma}_{m^{j1}_{1,\underline{a}_k}}(y_1)\,\bar{\sigma}_{m^{j2}_{2,\underline{a}_k}}(y_2)\,\bar{\sigma}_{m^{j3}_{3,\underline{a}_k}}(y_3) \tag{11}$$

4) The output $\hat{y}$ is given as [30]:

$$\hat{y} = y^T \mu \tag{12}$$

where, y and μ are:

$$y = \left[\underline{y}_1, \ldots, \underline{y}_M, \bar{y}_1, \ldots, \bar{y}_M\right]^T \tag{13}$$

$$\mu = \left[\underline{\mu}_1, \ldots, \underline{\mu}_M, \bar{\mu}_1, \ldots, \bar{\mu}_M\right]^T \tag{14}$$

where, M is rule numbers, and $\underline{\mu}_r$ and $\bar{\mu}_r$ are:

$$\bar{\mu}_r = \frac{\sum_{k=1}^{n_a} \bar{a}_k \frac{\bar{\upsilon}^r_{\bar{a}_k}}{\sum_{r=1}^{M}\left(\bar{\upsilon}^r_{\bar{a}_k} + \underline{\upsilon}^r_{\bar{a}_k}\right)}}{\sum_{k=1}^{n_a}\left(\bar{a}_k + \underline{a}_k\right)} + \frac{\sum_{j=1}^{n_a} \underline{a}_k \frac{\bar{\upsilon}^r_{\underline{a}_k}}{\sum_{r=1}^{M}\left(\bar{\upsilon}^r_{\underline{a}_k} + \underline{\upsilon}^r_{\underline{a}_k}\right)}}{\sum_{k=1}^{n_a}\left(\bar{a}_k + \underline{a}_k\right)}, \quad r = 1, \ldots, M \tag{15}$$

$$\underline{\mu}_r = \frac{\sum_{k=1}^{n_a} \bar{a}_k \frac{\underline{\upsilon}^r_{\bar{a}_k}}{\sum_{r=1}^{M}\left(\bar{\upsilon}^r_{\bar{a}_k} + \underline{\upsilon}^r_{\bar{a}_k}\right)}}{\sum_{k=1}^{n_a}\left(\bar{a}_k + \underline{a}_k\right)} + \frac{\sum_{j=1}^{n_a} \underline{a}_k \frac{\underline{\upsilon}^r_{\underline{a}_k}}{\sum_{r=1}^{M}\left(\bar{\upsilon}^r_{\underline{a}_k} + \underline{\upsilon}^r_{\underline{a}_k}\right)}}{\sum_{k=1}^{n_a}\left(\bar{a}_k + \underline{a}_k\right)}, \quad r = 1, \ldots, M \tag{16}$$

IV. MAIN RESULTS

The LC synthesis is partitioned as follows. First, consider the following nonlinear system

$$\begin{aligned} \dot{y}_1 &= y_2 \\ \dot{y}_2 &= f_2(y_1, y_2) + g_2(y_1, y_2) y_3 + F_2(y) \end{aligned} \tag{17}$$

where $F_2(y)$ is assumed to have the form of $F_2(y) = W_2^T \Phi_2(y)$ in which W_2 is a weight vector and $\Phi_2(y)$ will be computed via the IT3FLS. Furthermore, y_3 acts as a virtual signal and is designed as follows

$$
\begin{aligned}
y_3 &= \varphi_3(y_1, y_2) \\
&= \frac{1}{g_2(y_1, y_2)} \left(\begin{array}{l} -f_2(y_1, y_2) \\ -k_d \xi(y_1, y_2) \left(\psi(y_1, y_2) - r^2\right) - \eta(y_1, y_2) \end{array} \right. \\
&\quad \left. - \left(\frac{\partial \psi}{\partial y_2} \left(\psi(y_1, y_2) - r^2\right) \right) \left[\frac{1}{2a_2^2} \hat{\theta}_2 \Phi_2^T(y) \Phi_2(y) + \frac{1}{2} \right] \right)
\end{aligned} \tag{18}
$$

Now the following Lyapunov function targets the LC

$$
V_2 = \frac{1}{2} \left(\psi(y_1, y_2) - r^2\right)^2 + \frac{1}{2r_2} \tilde{\theta}_2^2 \tag{19}
$$

where r_2, a_2 are positive scalars considered as design parameters and $\tilde{\theta}_2 = \theta_2 - \hat{\theta}_2$ denotes the estimation error of the unknown parameter θ_2. It can be deduced that $V_2 = 0$ holds for $y \in L$ and the Lyapunov is positive definite. Indeed, for the second-order system $y_1 = x2, y_2 = F(y_1, y_2) + G(y_1, y_2)u(t)$ where $F(0, 0) = 0, G(y_1, y_2) \neq 0$, and $u(t) = v(y_1, y_2)$ denotes the control signal such that the defined LC of the structures $\digamma = y \in R^2, \psi(y_1, y_2) = r^2$ is produced in $y_1 - y_2$ plane of the control system. As an example, periodic solutions for $y_1(t) = A\sin(\omega t)$ and $y_2(t) = A\omega\cos(\omega t)$ are equivalent to the generation of the LC $\digamma = y \in R^2, \omega^2 y_1^2 + y_2^2 = (A\omega)^2$ in the $y_1 - y_2$ plane. The derivative of V_2 is:

$$
\begin{aligned}
\dot{V}_2 &= \left(\frac{\partial \psi}{\partial y_1} \left(\psi(y_1, y_2) - r^2\right) \right) \dot{y}_1 \\
&\quad + \left(\frac{\partial \psi}{\partial y_2} \left(\psi(y_1, y_2) - r^2\right) \right) \dot{y}_2 - \frac{1}{r_2} \tilde{\theta}_2 \dot{\hat{\theta}}_2 \\
&= \left(\frac{\partial \psi}{\partial y_1} \left(\psi(y_1, y_2) - r^2\right) \right) y_2 \\
&\quad + \left(\frac{\partial \psi}{\partial y_2} \left(\psi(y_1, y_2) - r^2\right) \right) \left[\begin{array}{l} f_2 - f_2 \\ - k_d \xi(y_1, y_2) \left(\psi(y_1, y_2) - r^2\right) - \eta(y_1, y_2) \\ - \left(\frac{\partial \psi}{\partial y_2} \left(\psi(y_1, y_2) - r^2\right) \right) \\ \cdot \left(\frac{1}{2a_2^2} \hat{\theta}_2 \Phi_2^T(y) \Phi_2(y) + \frac{1}{2} \right) \\ + F_2(y) \end{array} \right] - \frac{1}{r_2} \tilde{\theta}_2 \dot{\hat{\theta}}_2
\end{aligned} \tag{20}
$$

Based on the system model, one has

$$
\begin{aligned}
\dot{V}_2 &= \left(\frac{\partial \psi}{\partial y_1} \left(\psi(y_1, y_2) - r^2\right) \right) y_2 \\
&\quad - \left(\frac{\partial \psi}{\partial y_2} \left(\psi(y_1, y_2) - r^2\right) \right) k_d \xi(y_1, y_2) \\
&\quad - \left(\frac{\partial \psi}{\partial y_2} \eta(y_1, y_2) \left(\psi(y_1, y_2) - r^2\right) \right) \\
&\quad - \left\{ \begin{array}{l} \left(\frac{\partial \psi}{\partial y_2} \left(\psi(y_1, y_2) - r^2\right) \right)^2 \\ \cdot \left(\frac{1}{2a_2^2} \hat{\theta}_2 \Phi_2^T(y) \Phi_2(y) + \frac{1}{2} \right) \\ \cdot \frac{\partial \psi}{\partial y_2} \left(\psi(y_1, y_2) - r^2\right) F_2(y) \end{array} \right\} \\
&\quad - \frac{1}{r_2} \tilde{\theta}_2 \dot{\hat{\theta}}_2
\end{aligned} \tag{21}
$$

Now in order to deal with the uncertainties, it is assumed that

$$
F_2(y) = W_2^{*T} \Phi_2(y) + \delta_2(y); \quad |\delta_2(y)| \leq \varepsilon_2 \tag{22}
$$

where $W_2^* = \arg \min_{W_2} \sup_{y \in \Omega_y} |F_2(y) - W_2^{*T} \Phi_2(y)|$ denotes the ideal weights to be determined and $\delta_2(y)$ is the approximation error. By doing some calculations, we have

$$
\begin{aligned}
&\frac{\partial \psi}{\partial y_2} \left(\psi(y_1, y_2) - r^2\right) F_2(y) \\
&\leq \left| \frac{\partial \psi}{\partial y_2} \left(\psi(y_1, y_2) - r^2\right) \right| \left(\left\| W_2^* \right\| \left\| \Phi_2(y) \right\| + \varepsilon_2 \right) \\
&\leq \frac{1}{2a_2^2} \left(\frac{\partial \psi}{\partial y_2} \left(\psi(y_1, y_2) - r^2\right) \right)^2 \theta_2 \Phi_2^T(y) \Phi_2(y) \\
&\quad + \frac{a_2^2}{2} + \frac{1}{2} \left(\frac{\partial \psi}{\partial y_2} \left(\psi(y_1, y_2) - r^2\right) \right)^2 + \frac{\varepsilon_2^2}{2}
\end{aligned} \tag{23}
$$

in which $\theta_2 = \|W_2^*\|^2$. Moreover, one has

$$
\begin{aligned}
\dot{V}_2 &\leq -k_d \xi^2(y_1, y_2) \left(\psi(y_1, y_2) - r^2\right)^2 \\
&\quad + \frac{a_2^2}{2} + \frac{\varepsilon_2^2}{2} \\
&\quad + \frac{1}{r_2} \tilde{\theta}_2 \left[\begin{array}{l} \frac{r_2}{2a_2^2} \left(\frac{\partial \psi}{\partial y_2} \left(\psi(y_1, y_2) - r^2\right) \right)^2 \Phi_2^T(y) \Phi_2(y) \\ - \dot{\hat{\theta}}_2 \end{array} \right]
\end{aligned} \tag{24}
$$

The adaptive law $\dot{\hat{\theta}}_2$ is as follows

$$
\dot{\hat{\theta}}_2 = \frac{r_2}{2a_2^2} \left(\frac{\partial \psi}{\partial y_2} \left(\psi(y_1, y_2) - r^2\right) \right)^2 \Phi_2^T(y) \Phi_2(y) - \delta_2 \hat{\theta}_2 \tag{25}
$$

By considering the adaptation law in the upper bound of $\dot{V}_2$, the following results are acquired

$$
\begin{aligned}
\dot{V}_2 &\leq -k_d \xi^2(y_1, y_2) \left(\psi(y_1, y_2) - r^2\right)^2 \\
&\quad + \frac{a_2^2}{2} + \frac{\varepsilon_2^2}{2} + \frac{1}{r_2} \delta_2 \tilde{\theta}_2 \hat{\theta}_2
\end{aligned} \tag{26}
$$

Since the upper bound of $\dot{\tilde{V}}_2$ is continuous and positive with respect to the LC, the domain of attraction for the LC can be considered as $\Sigma = \{y : V_2 \leq c\}$ which is an invariant set, meaning that for $y_0 \in \Sigma$ trajectories remain within the set as $y \in \Sigma$. . By defining $z_3 = y_3 - \varphi_3$, one has

$$\begin{aligned} \dot{y}_1 &= y_2 \\ \dot{y}_2 &= f_2(y_1, y_2) + g_2(y_1, y_2)\varphi_3 + g_2(y_1, y_2)z_3 + F_2(y) \\ \dot{z}_3 &= f_3(y_1, y_2, y_3) + g_3(y_1, y_2, y_3)y_4 + F_3(y) - \dot{\varphi}_3 \end{aligned} \tag{27}$$

Now the Lyapunov function is modified as

$$V_3 = \frac{1}{2}\left(\psi - r^2\right)^2 + \frac{1}{2r_2}\tilde{\theta}_2^2 + \frac{1}{2r_3}\tilde{\theta}_3^2 + \frac{1}{2}z_3^2 \tag{28}$$

Taking the time derivative of (28) results in

$$\begin{aligned} \dot{V}_3 &= \frac{\partial V_2}{\partial y_1}\dot{y}_1 + \frac{\partial V_2}{\partial y_2}\dot{y}_2 - \frac{1}{r_3}\tilde{\theta}_3\dot{\hat{\theta}}_3 + z_3\dot{z}_3 \\ &\leq \dot{\tilde{V}}_2 + \frac{\partial V_2}{\partial y_2}g_2 z_3 - \frac{1}{r_3}\tilde{\theta}_3\dot{\hat{\theta}}_3 + z_3\left[f_3 + g_3 y_4 + F_3 - \dot{\varphi}_3\right] \end{aligned} \tag{29}$$

Similar to the previous step, one has

$$F_3(y) = W_3^{*T}\Phi_3(y) + \delta_3(y); \quad |\delta_3(y)| \leq \varepsilon_3 \tag{30}$$

with W_3^* as ideal weights and $\delta_3(y)$ as the approximation error. Furthermore, it is straightforward to acquire the following inequalities

$$\begin{aligned} z_3F_3 &\leq |z_3|\left(\|W_3^*\|\|\Phi_3(y)\| + \varepsilon_3\right) \\ &\leq \frac{1}{2a_3^2}z_3^2\theta_3\Phi_3^T(y)\,\Phi_3(y) + \frac{a_3^2}{2} + \frac{z_3^2}{2} + \frac{\varepsilon_3^2}{2} \end{aligned} \tag{31}$$

which results in

$$\begin{aligned} \dot{V}_3 \leq \dot{\tilde{V}}_2 &+ \frac{\partial V_2}{\partial z_2}g_2 z_3 - \frac{1}{r_3}\tilde{\theta}_3\dot{\hat{\theta}}_3 + z_3\left[f_3 + g_3 y_4 - \dot{\varphi}_3\right] \\ &+ \frac{1}{2a_3^2}z_3^2\theta_3\Phi_3^T(y)\,\Phi_3(y) + \frac{a_3^2}{2} + \frac{z_3^2}{2} + \frac{\varepsilon_3^2}{2} \end{aligned} \tag{32}$$

Consider the virtual input as

$$\begin{aligned} y_4 &= \varphi_4 \\ &= \frac{1}{g_3}\begin{bmatrix} -f_3 + \dot{\varphi}_3 - c_3 z_3 \\ -\frac{1}{2a_3^2}z_3\hat{\theta}_3\Phi_3^T(y)\Phi_3(y) - \frac{\partial V_2}{\partial y_2}g_2 \end{bmatrix} \end{aligned} \tag{33}$$

Then, the following holds

$$\begin{aligned} \dot{V}_3 &\leq \dot{\tilde{V}}_2 \\ &\quad + \frac{1}{2a_3^2}z_3^2\theta_3\Phi_3^T(y)\Phi_3(y) + \frac{a_3^2}{2} + \frac{z_3^2}{2} + \frac{\varepsilon_3^2}{2} \\ &\quad - \frac{1}{r_3}\tilde{\theta}_3\dot{\hat{\theta}}_3 - c_3 z_3^2 \\ &\leq \dot{\tilde{V}}_2 + \frac{a_3^2}{2} + \frac{z_3^2}{2} + \frac{\varepsilon_3^2}{2} \\ &\quad - c_3 z_3^2 + \frac{1}{r_3}\tilde{\theta}_3\left(\frac{1}{2a_3^2}z_3^2\Phi_3^T(y)\Phi_3(y) - \dot{\hat{\theta}}_3\right) \end{aligned} \tag{34}$$

As a result, the adaptation policy is as follows

$$\dot{\hat{\theta}}_3 = \frac{r_3}{2a_3^2}z_3^2\Phi_3^T(y)\,\Phi_3(y) - \delta_3\hat{\theta}_3 \tag{35}$$

Considering (54), the upper bound of $\dot{V}_3$ in (53) is acquired as

$$\dot{V}_3 \leq \dot{\tilde{V}}_2 + \frac{a_3^2}{2} + \frac{z_3^2}{2} + \frac{\varepsilon_3^2}{2} + \frac{1}{r_3}\delta_3\tilde{\theta}_3\hat{\theta}_3 - c_3 z_3^2 = \dot{\tilde{V}}_3 \tag{36}$$

By defining $z_4 = y_4 - \varphi_4$ it can be deduced that

$$\begin{aligned} \dot{y}_1 &= y_2 \\ \dot{y}_2 &= f_2(y_1, y_2) + g_2(y_1, y_2)\varphi_3 \\ &\quad + g_2(y_1, y_2)z_3 + F_2(y) \\ \dot{z}_3 &= f_3(y_1, y_2, y_3) + g_3(y_1, y_2, y_3)\varphi_4 \\ &\quad + F_3(y) + g_3(y_1, y_2, y_3)z_4 \\ \dot{z}_4 &= f_4(y_1, y_2, y_3, y_4) + g_4(y_1, y_2, y_3, y_4)y_5 \\ &\quad + F_4(y) - \dot{\varphi}_4 \end{aligned} \tag{37}$$

We reform the Lyapunov candidate as follows

$$V_4 = V_3 + \frac{1}{2r_4}\tilde{\theta}_4^2 + \frac{1}{2}z_4^2 \tag{38}$$

Taking the time derivative of V_4 gives rise to

$$\dot{V}_4 = \frac{\partial V_3}{\partial y_1}\dot{y}_1 + \frac{\partial V_3}{\partial y_2}\dot{y}_2 + \frac{\partial V_3}{\partial z_3}\dot{z}_3 - \frac{1}{r_4}\tilde{\theta}_4\dot{\hat{\theta}}_4 + z_4\dot{z}_4 \tag{39}$$

Similar to the previous steps, one has

$$\dot{V}_4 \leq \dot{\tilde{V}}_3 + \frac{\partial V_3}{\partial z_3}g_3 z_4 - \frac{1}{r_4}\tilde{\theta}_4\dot{\hat{\theta}}_4 + z_4\left[f_4 + g_4 y_5 + F_5 - \dot{\varphi}_4\right] \tag{40}$$

Next, the following inequality is achieved

$$\begin{aligned} z_4F_4 &\leq |z_4|\left(\|W_4^*\|\|\Phi_4(y)\| + \varepsilon_4\right) \\ &\leq \frac{1}{2a_4^2}z_4^2\theta_4\Phi_4^T(y)\,\Phi_4(y) + \frac{a_4^2}{2} + \frac{z_4^2}{2} + \frac{\varepsilon_4^2}{2} \end{aligned} \tag{41}$$

Therefore, it can be deduced that

$$\begin{aligned} \dot{V}_4 \leq \dot{\tilde{V}}_3 &+ \frac{\partial V_3}{\partial z_3}g_3 z_4 - \frac{1}{r_4}\tilde{\theta}_4\dot{\hat{\theta}}_4 + z_4\left[f_4 + g_4 y_5 - \dot{\varphi}_4\right] \\ &+ \frac{1}{2a_4^2}z_4^2\theta_4\Phi_4^T(y)\,\Phi_4(y) + \frac{a_4^2}{2} + \frac{z_4^2}{2} + \frac{\varepsilon_4^2}{2} \end{aligned} \tag{42}$$

Now by designing a virtual input as

$$\begin{aligned} y_5 &= \varphi_5 \\ &= \frac{1}{g_4}\begin{bmatrix} -f_4 + \dot{\varphi}_4 - c_4 z_4 \\ -\frac{1}{2a_4^2}z_4\hat{\theta}_4\Phi_4^T(X_4)\Phi_4(X_4) - \frac{\partial V_3}{\partial z_3}g_3 \end{bmatrix} \end{aligned} \tag{43}$$

and the adaptive law as

$$\dot{\hat{\theta}}_4 = \frac{r_4}{2a_4^2}z_4^2\Phi_4^T(y)\,\Phi_4(y) - \delta_4\hat{\theta}_4 \tag{44}$$

leads to

$$\dot{V}_4 \leq \dot{\tilde{V}}_3 + \frac{a_4^2}{2} + \frac{z_4^2}{2} + \frac{\varepsilon_4^2}{2} + \frac{1}{r_4}\delta_4\tilde{\theta}_4\hat{\theta}_4 - c_4 z_4^2 \tag{45}$$

As a result we can partition the synthesis into two parts. First, for $q = 2$, we have

$$u_q = \frac{1}{g_2(y_1, y_2)}\Bigg(-f_2(y_1, y_2) - k_d\xi(y_1, y_2)\left(\psi(y_1, y_2) - r^2\right) - \eta(y_1, y_2) - \left(\frac{\partial\psi}{\partial y_2}\left(\psi(y_1, y_2)-r^2\right)\right)\left[\frac{1}{2a_2^2}\hat{\theta}_2\Phi_2^T(y)\Phi_2(y)+\frac{1}{2}\right]\Bigg) \tag{46}$$

with the Lyapunov function as

$$V_2 = \frac{1}{2}\left(\psi(y_1, y_2) - r^2\right)^2 + \frac{1}{2r_2}\tilde{\theta}_2^2 \tag{47}$$

Second, for $q \geq 3$, it can be deduced that

$$u_q = \frac{1}{g_q} - f_q + \dot{\varphi}_q - c_q z_q - \frac{1}{2a_q^2} z_q\hat{\theta}_q\Phi_q^T(y)\Phi_q(y) - \frac{\partial V_{q-1}}{\partial z_{q-1}} g_{q-1} \tag{48}$$

And the Lyapunov for the n-th step as follows

$$V_n = \frac{1}{2}\left(\psi(y_1, y_2) - r^2\right)^2 + \frac{1}{2}\sum_{j=3}^{n} z_j^2 + \frac{1}{2}\sum_{j=2}^{n}\frac{1}{2r_j}\tilde{\theta}_j^2 \tag{49}$$

By applying the control signal to the system we have

$$\dot{V}_n \leq -k_d\xi^2(y_1, y_2)\left(\psi(y_1, y_2) - r^2\right)^2 + \sum_{j=2}^{n}\left(\frac{\delta_j}{2r_j}\theta_j^2 + \frac{1}{2}\varepsilon_j^2 + \frac{1}{2}\alpha_j^2\right) \tag{50}$$

This inequality satisfies that ensures that trajectories remain bounded, ensuring that closed-loop trajectories converge to the neighbourhood of the determined LC. By developing the approximation quality of unknown functions, the trajectories converge quickly and accurately to the LC.

V. CALCULATION REDUCTION

Lemma 1: The Levent's first order differentiator has the following equations

$$\begin{aligned}\dot{\alpha}_0(t) &= -L_0|\alpha_0(t) - \varphi(t)|^{\frac{1}{2}} sign(\alpha_0(t) - \varphi(t)\,) + \alpha_1(t)\\ \dot{\alpha}_1(t) &= -L_1 sign(\alpha_0(t) - \varphi(t)\,)\end{aligned} \tag{51}$$

where $\varphi(t)$ and $\alpha_0(t), \alpha_1(t)$ denotes input and outputs of the differentiator and also L_0, L_1 are positive constants.

Since the computation of $\dot{\varphi}_i$ is an unsurmountable problem in practice, in this section we modify the synthesis such that the calculation load is reduced. To tackle this issue and based on the Lemma 1 with $\alpha_{2,0} = \varphi_3(t)$, $\alpha_{2,1} = \dot{\varphi}_3(t)$, $\mu_2 = \alpha_{2,1} - \dot{\varphi}_3(t)$, $|\mu_2| \leq \bar{\mu}_2$, the virtual input is designed as

$$\begin{aligned} y_4 &= \varphi_4 \\ &= \frac{1}{g_3}\left[\begin{array}{l} -f_3 + \alpha_{2,1} - c_3 z_3 \\ -\frac{1}{2a_3^2} z_3\hat{\theta}_3\Phi_3^T(y)\Phi_3(y) - \frac{\partial V_2}{\partial y_2} g_2 \end{array}\right]\end{aligned} \tag{52}$$

Therefore the following inequality holds

$$\begin{aligned}\dot{V}_3 &\leq \dot{\bar{V}}_2 + \frac{1}{2a_3^2} z_3^2\theta_3\Phi_3^T(y)\Phi_3(y) \\ &\quad + \frac{a_3^2}{2} + \frac{z_3^2}{2} + \frac{\varepsilon_3^2}{2} - \frac{1}{r_3}\tilde{\theta}_3\dot{\hat{\theta}}_3 - c_3 z_3^2 \\ &\quad + z_3\left(\alpha_{2,1} - \dot{\varphi}_3\right) \\ &\leq \dot{\bar{V}}_2 + \frac{a_3^2}{2} + \frac{z_3^2}{2} + \frac{\varepsilon_3^2}{2} \\ &\quad - c_3 z_3^2 + |z_3|\bar{\mu}_2 \\ &\quad + \frac{1}{r_3}\tilde{\theta}_3\left(\frac{1}{2a_3^2} z_3^2\Phi_3^T(y)\Phi_3(y) - \dot{\hat{\theta}}_3\right)\end{aligned} \tag{53}$$

And the adaptation policy is obtained as

$$\dot{\hat{\theta}}_3 = \frac{r_3}{2a_3^2} z_3^2\Phi_3^T(y)\,\Phi_3(y)\; - \delta_3\hat{\theta}_3 \tag{54}$$

Considering (54), the upper bound of $\dot{V}_3$ in (53) is acquired as

$$\begin{aligned}\dot{V}_3 &\leq \dot{\bar{V}}_2 + \frac{a_3^2}{2} + \frac{z_3^2}{2} + \frac{\varepsilon_3^2}{2} \\ &\quad + \frac{1}{r_3}\delta_3\tilde{\theta}_3\hat{\theta}_3 - c_3 z_3^2 + |z_3|\bar{\mu}_2 \\ &= \dot{\bar{V}}_3 + |z_3|\bar{\mu}_2\end{aligned} \tag{55}$$

Now by considering $z_4 = y_4 - \varphi_4$, one has

$$\begin{aligned}\dot{y}_1 &= y_2 \\ \dot{y}_2 &= f_2(y_1, y_2) + g_2(y_1, y_2)\varphi_3 + g_2(y_1, y_2)z_3 \\ &\quad + F_2(y) \\ \dot{z}_3 &= f_3(y_1, y_2, y_3) + g_3(y_1, y_2, y_3)\varphi_4 \\ &\quad + F_3(y) + g_3(y_1, y_2, y_3)z_4 \\ \dot{z}_4 &= f_4(y_1, y_2, y_3, y_4) + g_4(y_1, y_2, y_3, y_4)y_5 \\ &\quad + F_4(y) - \dot{\varphi}_4\end{aligned} \tag{56}$$

Moreover, the Lyapunov function is employed as

$$V_4 = V_3 + \frac{1}{2r_4}\tilde{\theta}_4^2 + \frac{1}{2}z_4^2 \tag{57}$$

The time derivative of V_4 is acquired as

$$\dot{V}_4 = \frac{\partial V_3}{\partial y_1}\dot{y}_1 + \frac{\partial V_3}{\partial y_2}\dot{y}_2 + \frac{\partial V_3}{\partial z_3}\dot{z}_3 - \frac{1}{r_4}\tilde{\theta}_4\dot{\hat{\theta}}_4 + z_4\dot{z}_4 \tag{58}$$

Similar to the previous steps, it can be achieved that

$$\begin{aligned}\dot{V}_4 \leq \dot{\bar{V}}_3 + \frac{\partial V_3}{\partial z_3} g_3 z_4 - \frac{1}{r_4}\tilde{\theta}_4\dot{\hat{\theta}}_4 \\ + z_4\left[f_4 + g_4 y_5 + F_5 - \dot{\varphi}_4\right]\end{aligned} \tag{59}$$

Furthermore, we have

$$\begin{aligned} z_4 F_4 &\leq |z_4|\left(\|W_4^*\|\|\Phi_4(y)\,\| + \varepsilon_4\right) \\ &\leq \frac{1}{2a_4^2} z_4^2\theta_4\Phi_4^T(y)\,\Phi_4(y)\; + \frac{a_4^2}{2} + \frac{z_4^2}{2} + \frac{\varepsilon_4^2}{2}\end{aligned} \tag{60}$$

which leads to

$$\dot{V}_4 \leq \dot{\tilde{V}}_3 + \frac{\partial V_3}{\partial z_3} g_3 z_4 - \frac{1}{r_4}\tilde{\theta}_4\dot{\hat{\theta}}_4 + z_4\left[f_4 + g_4 y_5 - \dot{\varphi}_4\right] + \frac{1}{2a_4^2} z_4^2 \theta_4 \Phi_4^T(y)\,\Phi_4(y) + \frac{a_4^2}{2} + \frac{z_4^2}{2} + \frac{\varepsilon_4^2}{2} \tag{61}$$

Based on a virtual input as follows

$$y_5 = \varphi_5 = \frac{1}{g_4}\cdot\begin{bmatrix} -f_4 + \alpha_{3,1} - c_4 z_4 \\ -\frac{1}{2a_4^2} z_4 \hat{\theta}_4 \Phi_4^T(X_4)\Phi_4(X_4) - \frac{\partial V_3}{\partial z_3} g_3 \end{bmatrix} \tag{62}$$

and the adaptive law as

$$\dot{\hat{\theta}}_4 = \frac{r_4}{2a_4^2} z_4^2 \Phi_4^T(y)\,\Phi_4(y) - \delta_4\hat{\theta}_4 \tag{63}$$

one has

$$\dot{V}_4 \leq \dot{\tilde{V}}_3 + \frac{a_4^2}{2} + \frac{z_4^2}{2} + \frac{\varepsilon_4^2}{2} + \frac{1}{r_4}\delta_4\tilde{\theta}_4\hat{\theta}_4 - c_4 z_4^2 + |z_4|\bar{\mu}_3 \tag{64}$$

To conclude, the synthesis can be defined in the framework of the two parts. First, for $q = 2$, one has

$$u_q = \frac{1}{g_2(y_1, y_2)} \cdot \left(\begin{array}{l} -f_2(y_1,y_2) - k_d \xi(y_1,y_2)\left(\gamma(y_1,y_2) - r^2\right) \\ -\eta(y_1,y_2) - \left[\frac{\partial \gamma}{\partial y_2}\left(\gamma(y_1,y_2) - r^2\right)\right] \\ \cdot\left[\frac{1}{2a_2^2}\hat{\theta}_2 \Phi_2^T(y)\Phi_2(y) + \frac{1}{2}\right] \end{array} \right) \tag{65}$$

with the Lyapunov function as

$$V_2 = \frac{1}{2}\left(\gamma(y_1,y_2) - r^2\right)^2 + \frac{1}{2r_2}\tilde{\theta}_2^2 \tag{66}$$

Second, for $q \geq 3$, it can be deduced that

$$u_q = \frac{1}{g_q}\cdot\begin{bmatrix} -f_q + \alpha_{n-1,1} - c_q z_q \\ -\frac{1}{2a_q^2} z_q \hat{\theta}_q \Phi_q^T(y)\Phi_q(y) - \frac{\partial V_{q-1}}{\partial z_{q-1}} g_{q-1} \end{bmatrix} \tag{67}$$

And the Lyapunov for the n-th step as follows

$$V_n = \frac{1}{2}\left(\gamma(y_1,y_2) - r^2\right)^2 + \frac{1}{2}\sum_{j=3}^{n} z_j^2 + \frac{1}{2}\sum_{j=2}^{n}\frac{1}{2r_j}\tilde{\theta}_j^2 \tag{68}$$

Moreover, implementing the control signal for the system gives rise to

$$\dot{V}_n \leq -k_d \xi^2(y_1,y_2)\left(\gamma(y_1,y_2) - r^2\right)^2 + \sum_{j=2}^{n}\left(\frac{\delta_j}{2r_j}\theta_j^2 + \frac{1}{2}\varepsilon_j^2 + \frac{1}{2}\alpha_j^2\right) + \sum_{j=2}^{n-1}|z_{j+1}|\bar{\mu}_j \tag{69}$$

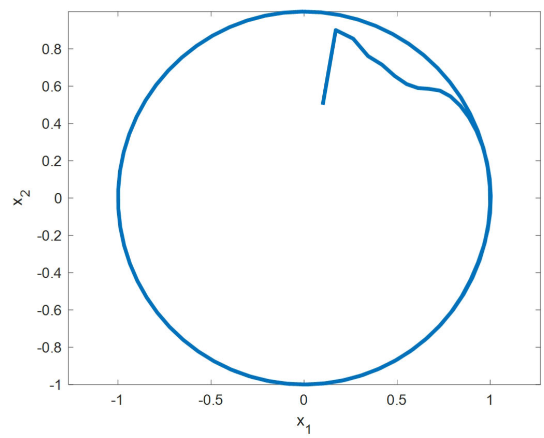

FIGURE 4. The convergence efficiency of generated LC.

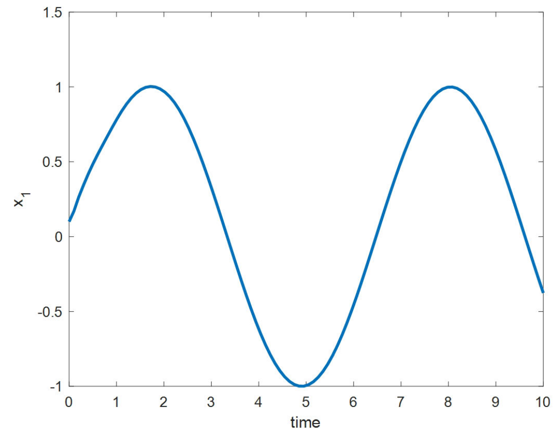

FIGURE 5. The trajectory of y1.

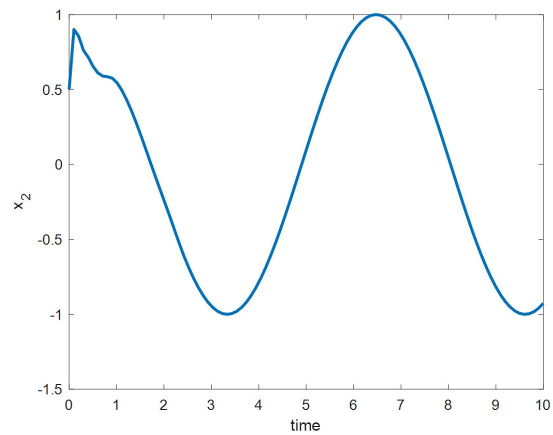

FIGURE 6. The trajectory of y2.

VI. SIMULATION RESULTS

Example 1: Consider the model of the single-link flexible joint robot system as follows:

$$\dot{y}_1 = y_2$$
$$\dot{y}_2 = \sin y_1 - 7.5\, y_1 + y_3 + F_2(t, y)$$

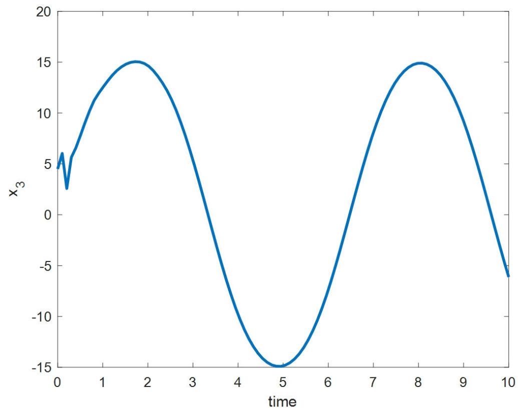

FIGURE 7. The trajectory of y3.

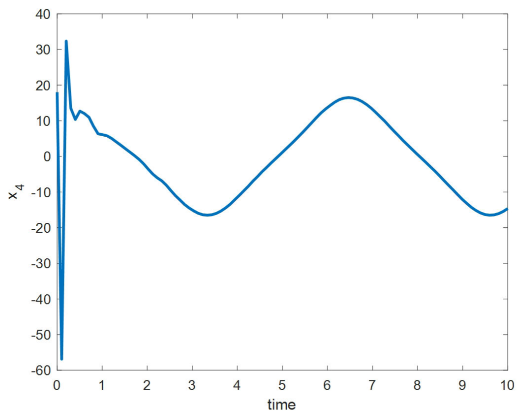

FIGURE 8. The trajectory of y4.

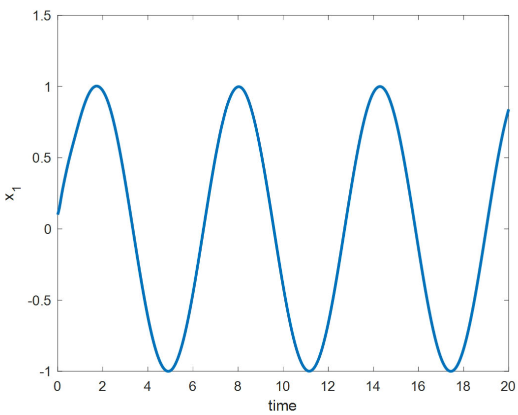

FIGURE 9. The of y1 with 70% loss of effectiveness.

$$\begin{aligned} \dot{y}_3 &= y_4 \\ \dot{y}_4 &= y_3 + 225y_1 + 15\,u + F_4(t, y) \end{aligned} \tag{70}$$

where $F_2(t, y)/F_4(t, y)$ are unknown functions. The aim is to generate a LC of the form $L = \{y \in D \subseteq \mathbb{R}^2 y_1^2 + y_2^2 = 1\}$ in the $y_1 - y_2$ plane. By the introduced method, the stable LC is designed and demonstrated in Fig. 4. Moreover, trajectories and adaption parameters are portrayed in Figs. 5–8. From simulations it is confirmed that closed-loop signals in the presence of unknown functions converge to an appropriate

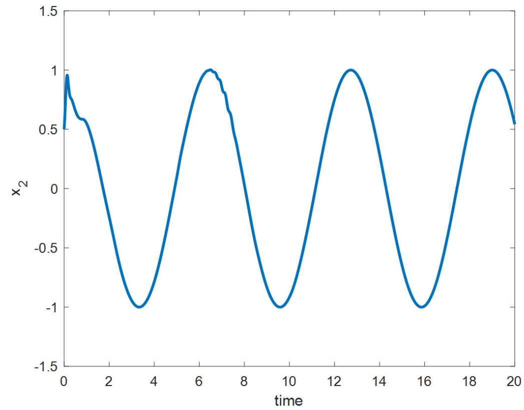

FIGURE 10. The trajectory of y2 with 70% loss of effectiveness.

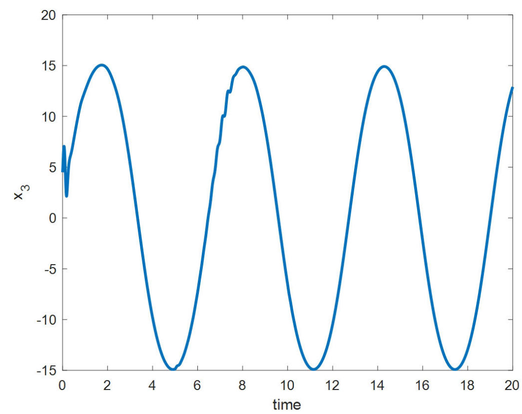

FIGURE 11. The trajectory of y3 with 70% loss of effectiveness.

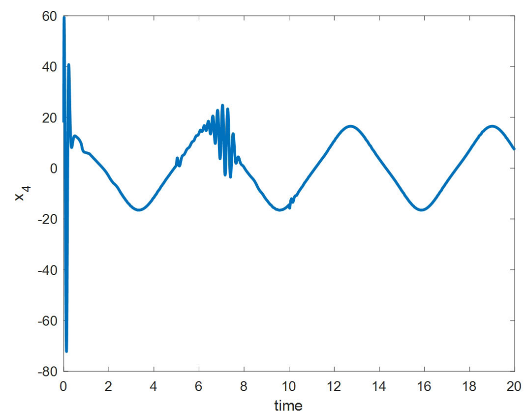

FIGURE 12. The trajectory of y4 with 70% loss of effectiveness.

LC, resulting in creating oscillatory behaviours in the state trajectories. Furthermore, simulations show that the effects of uncertainties are mitigated, resulting in desirable responses. Now consider the following dynamic

$$\begin{aligned} \dot{y}_1 &= y_2 \\ \dot{y}_2 &= \phi_2 \sin y_1 - 7.5\, y_1 + y_3 + F_2(t, y) \\ \dot{y}_3 &= y_4 \\ \dot{y}_4 &= \phi_4 y_3 + 225y_1 + 15\,u + F_4(t, y) \end{aligned} \tag{71}$$

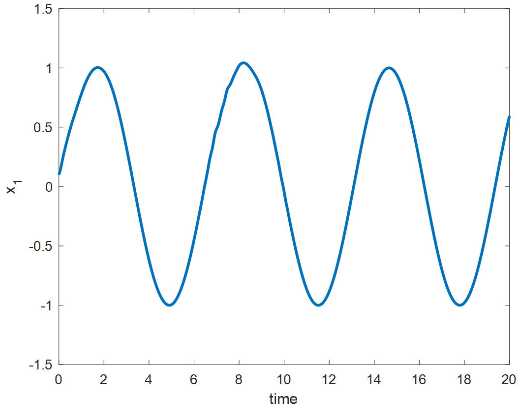

FIGURE 13. The trajectory of y1 with 80% loss of effectiveness.

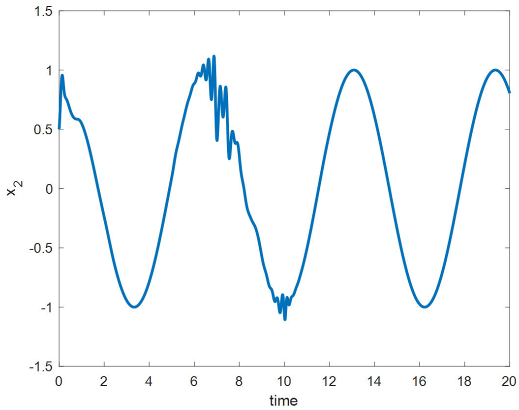

FIGURE 14. The trajectory of y2 with 80% loss of effectiveness.

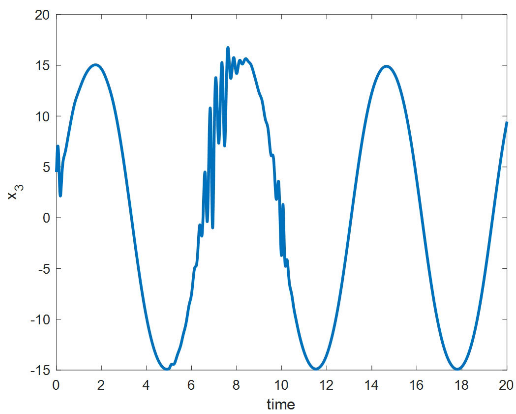

FIGURE 15. The trajectory of y3 with 80% loss of effectiveness.

To compare the results with conventional method of [10] in our simulations we consider

$$\begin{aligned} \phi_2 &\in [-20, 20], \\ \phi_4 &\in [-20, 20], \\ F_2(t, y) &= (\sin(t + \pi/4)) + \tanh(y_2), \\ F_4(t, y) &= (\sin(t + \pi/3)) + \tanh(y_4) \end{aligned} \tag{72}$$

and Fig. 5 verifies the priority of the approach of this paper. It is obvious that the conventional method fails to acquire the convergence in the presence of considered values for

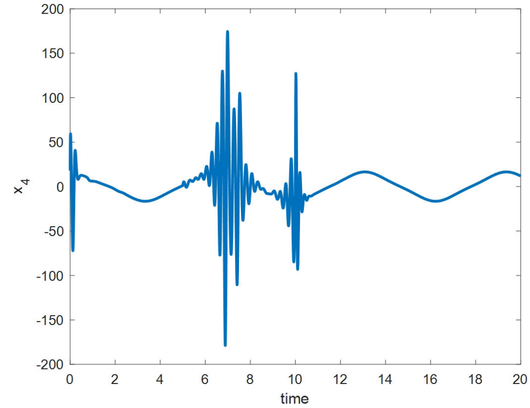

FIGURE 16. The trajectory of y4 with 80% loss of effectiveness.

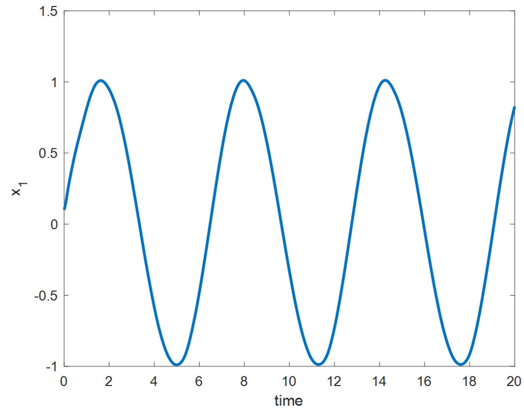

FIGURE 17. The trajectory of y1 in the presence of noise.

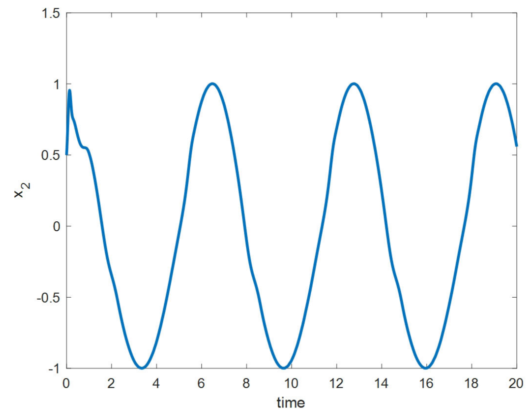

FIGURE 18. The trajectory of y2 in the presence of noise.

$F_2(t, y)/F_4(t, y)$ while the control method of this paper tackles uncertainties and trajectories converge to the desired LC. To explore the effectiveness of the $T3$ compared to $T2$ proposed in [34], we conduct simulations for the unknown external disturbances

$$\begin{aligned} \phi_2 &\in [-40, 40], \\ \phi_4 &\in [-40, 40], \\ F_2(t) &= 2(\sin(t + \pi/4)) + 2\tanh(y_2), \\ F_4(t) &= 2(\sin(t + \pi/3)) + 2\tanh(y_4) \end{aligned} \tag{73}$$

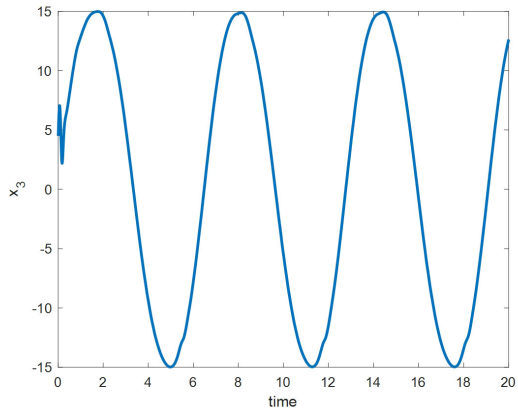

FIGURE 19. The trajectory of y3 in the presence of noise.

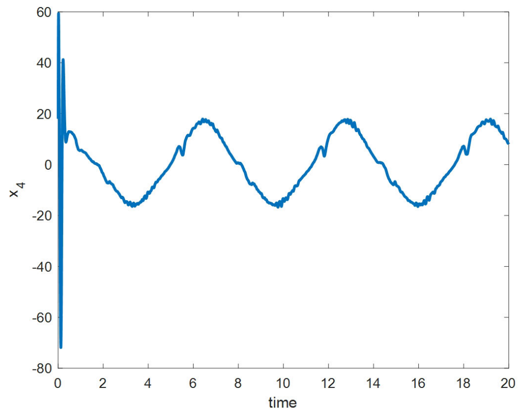

FIGURE 20. The trajectory of y4 in the presence of noise.

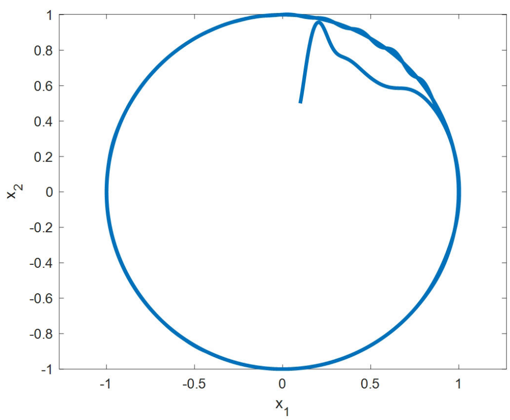

FIGURE 21. The convergence of trajectories to the generated LC with 70% loss of effectiveness.

It is noticeable that the method of method of [10] is not able to tackle uncertainties with such range of variations. It can be seen from Fig. 6 that the T3 FLS used in the control method of this paper is able to tackle uncertainties. From the comparison analysis, trajectories of the controlled system suggested by this paper well converge to LC and the can be seen that the convergence rate is appropriate. Moreover, the transient response is more smooth, verifying that the suggested control method enhanced the transient response and convergence speed remarkably. Moreover, the accuracy of the proposed scheme is much higher than employing T2 fuzzy logic system proposed in. It is noticeable that previous methods require specific bound for ϕ_2/ϕ_4 while the method of this paper approximate uncertainties due to the terms $\phi_2 \sin y_1/\phi_4 y_3$ and $F_2(t, y)/F_4(t, y)$ by advanced fuzzy logic systems.

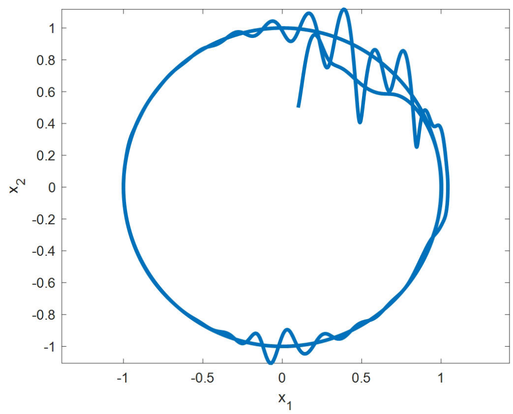

FIGURE 22. The convergence of trajectories to the generated LC with 80% loss of effectiveness.

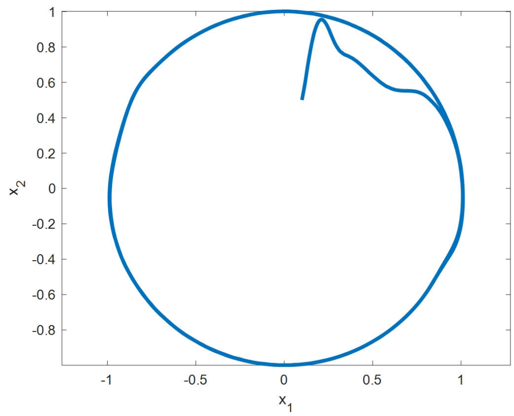

FIGURE 23. The convergence of trajectories to the generated LC in the presence of noise.

To illustrate the usefulness of the proposed approach against faulty control signal and additive white Gaussian noise, two scenarios are simulated. First it is shown that in Figs. 9–16, the suggested method is able to cope with 70% and 80% loss of effectiveness, corroborating the fault-tolerant capability of the suggested method. Then, the effect of noise is analyzed and demonstrated in Figs. 17–20 while the stable LC is designed and demonstrated in Figs. 21–23. From simulations, despite the inappropriate effects of fault which deteriorate the efficiency of the actuator, the T3-based FC benefited from the adaptive structure of modern T3 FLS, compensates loss of effectiveness and the improves the robustness.

VII. CONCLUSION

This paper dealt with the design of the LC for nonlinear systems with uncertainties. Based on a advanced fuzzy logic theorem, the synthesize improved, resulting in oscillatory behaviours of trajectories. Moreover, the backstepping technique was employed. From simulations it is confirmed that trajectories in the presence of unknown functions converge to the desired LC, resulting in creating oscillatory behaviours in the state trajectories. Furthermore, simulations show that the effects of uncertainties are mitigated, resulting in desirable responses of the closed-loop system. Future work will be imposing the constraints on the control signals and considering actuator saturations. This constraint is a physical challenging issue required further attention. Another improvement is developing an algorithm to determine the value of design parameters in an optimized way.

REFERENCES

[1] O. Miguel-Escrig, J.-A. Romero-Pérez, J. Sánchez-Moreno, and S. Dormido, "Characterization of limit cycle oscillations induced by fixed threshold samplers," *IEEE Access*, vol. 10, pp. 62581–62596, 2022.

[2] J. Aracil, F. Gordillo, and E. Ponce, "Stabilization of oscillations through backstepping in high-dimensional systems," *IEEE Trans. Autom. Control*, vol. 50, no. 5, pp. 705–710, May 2005.

[3] G. Garofalo and C. Ott, "Energy based limit cycle control of elastically actuated robots," *IEEE Trans. Autom. Control*, vol. 62, no. 5, pp. 2490–2497, May 2017.

[4] M. Azhdari and T. Binazadeh, "Uniformly ultimately bounded tracking control of sandwich systems with nonsymmetric sandwiched dead-zone nonlinearity and input saturation constraint," *J. Vib. Control*, vol. 28, nos. 9–10, pp. 1109–1125, May 2022.

[5] M. Azhdari and T. Binazadeh, "A novel adaptive SMC strategy for sustained oscillations in nonlinear sandwich systems based on stable limit cycle approach," *Chaos, Solitons Fractals*, vol. 161, Aug. 2022, Art. no. 112330.

[6] A. R. Hakimi, M. Azhdari, and T. Binazadeh, "Limit cycle oscillator in nonlinear systems with multiple time delays," *Chaos, Solitons Fractals*, vol. 153, Dec. 2021, Art. no. 111454.

[7] A. Hakimi and T. Binazadeh, "Inducing sustained oscillations in a class of nonlinear discrete time systems," *J. Vib. Control*, vol. 24, no. 6, pp. 1162–1170, Mar. 2018.

[8] A. R. Hakimi and T. Binazadeh, "Robust limit cycle control in a class of nonlinear discrete-time systems," *Int. J. Syst. Sci.*, vol. 49, no. 15, pp. 3108–3116, Nov. 2018.

[9] N. Oliveira, K. Kienitz, and E. Misawa, "A describing function approach to limit cycle controller design," in *Proc. Amer. Control Conf.*, 2006, p. 6.

[10] A. R. Hakimi and T. Binazadeh, "Generation of stable oscillations in uncertain nonlinear systems with matched and unmatched uncertainties," *Int. J. Control*, vol. 92, no. 1, pp. 163–174, Jan. 2019.

[11] T. Binazadeh and M. Karimi, "Robust stable limit cycle generation in multi-input mechanical systems," *Robotica*, vol. 39, no. 7, pp. 1316–1327, Jul. 2021.

[12] D. A. Haghighi and S. Mobayen, "Design of an adaptive super-twisting decoupled terminal sliding mode control scheme for a class of fourth-order systems," *ISA Trans.*, vol. 75, pp. 216–225, Apr. 2018.

[13] L. Magni, G. De Nicolao, R. Scattolini, and F. Allgöwer, "Robust model predictive control for nonlinear discrete-time systems," *Int. J. Robust Nonlinear Control*, vol. 13, nos. 3–4, pp. 229–246, Mar. 2003.

[14] A. Taghieh and M. H. Shafiei, "Observer-based robust model predictive control of switched nonlinear systems with time delay and parametric uncertainties," *J. Vib. Control*, vol. 27, nos. 17–18, pp. 1939–1955, Sep. 2021.

[15] M. S. Mahmoud, "Robust H_∞ control of linear neutral systems," *Automatica*, vol. 36, no. 5, pp. 757–764, 2000.

[16] T.-L. Le and V.-B. Ngo, "The synchronization of hyperchaotic systems using a novel interval type-2 fuzzy neural network controller," *IEEE Access*, vol. 10, pp. 105966–105982, 2022.

[17] M. Rabah, H. Haghbayan, E. Immonen, and J. Plosila, "An AI-in-loop fuzzy-control technique for UAV's stabilization and landing," *IEEE Access*, vol. 10, pp. 101109–101123, 2022.

[18] A. Mohammadzadeh and O. Kaynak, "A novel fractional-order fuzzy control method based on immersion and invariance approach," *Appl. Soft Comput.*, vol. 88, Mar. 2020, Art. no. 106043.

[19] Y. Yang, Y. Niu, and H. R. Karimi, "Dynamic learning control design for interval type-2 fuzzy singularly perturbed systems: A component-based event-triggering protocol," *Int. J. Robust Nonlinear Control*, vol. 32, no. 5, pp. 2518–2535, Mar. 2022.

[20] M. Rabah, A. Rohan, S. A. S. Mohamed, and S.-H. Kim, "Autonomous moving target-tracking for a UAV quadcopter based on fuzzy-PI," *IEEE Access*, vol. 7, pp. 38407–38419, 2019.

[21] J.-X. Zhang and G.-H. Yang, "Distributed fuzzy adaptive output-feedback control of unknown nonlinear multiagent systems in strict-feedback form," *IEEE Trans. Cybern.*, vol. 52, no. 6, pp. 5607–5617, Jun. 2022.

[22] R. Martínez, O. Castillo, and L.T. Aguilar, "Optimization of interval type-2 fuzzy logic controllers for a perturbed autonomous wheeled mobile robot using genetic algorithms," *Inf. Sci.*, vol. 179, no. 13, pp. 2158–2174, Jun. 2009.

[23] O. Castillo, L. Amador-Angulo, J. R. Castro, and M. Garcia-Valdez, "A comparative study of type-1 fuzzy logic systems, interval type-2 fuzzy logic systems and generalized type-2 fuzzy logic systems in control problems," *Inf. Sci.*, vol. 354, pp. 257–274, Aug. 2016.

[24] O. Castillo, H. Neyoy, J. Soria, P. Melin, and F. Valdez, "A new approach for dynamic fuzzy logic parameter tuning in ant colony optimization and its application in fuzzy control of a mobile robot," *Appl. Soft Comput.*, vol. 28, pp. 150–159, Mar. 2015.

[25] T. Kumbasar, I. Eksin, M. Guzelkaya, and E. Yesil, "Type-2 fuzzy model based controller design for neutralization processes," *ISA Trans.*, vol. 51, no. 2, pp. 277–287, Mar. 2012.

[26] Y. Chen, "Study on sampling based discrete Nie–Tan algorithms for computing the centroids of general type-2 fuzzy sets," *IEEE Access*, vol. 7, pp. 156984–156992, 2019.

[27] Y. Chen, "Comparison study of iterative algorithms for center-of-sets type-reduction of Takagi Sugeno Kang type general type-2 fuzzy logic systems," *IEEE Access*, vol. 10, pp. 105693–105701, 2022.

[28] Y. Cao, A. Raise, A. Mohammadzadeh, S. Rathinasamy, S. S. Band, and A. Mosavi, "Deep learned recurrent type-3 fuzzy system: Application for renewable energy modeling/prediction," *Energy Rep.*, vol. 7, pp. 8115–8127, Nov. 2021.

[29] M.-W. Tian, S.-R. Yan, A. Mohammadzadeh, J. Tavoosi, S. Mobayen, R. Safdar, W. Assawinchaichote, M. T. Vu, and A. Zhilenkov, "Stability of interval type-3 fuzzy controllers for autonomous vehicles," *Mathematics*, vol. 9, no. 21, p. 2742, Oct. 2021.

[30] A. Mohammadzadeh, M. H. Sabzalian, and W. Zhang, "An interval type-3 fuzzy system and a new online fractional-order learning algorithm: Theory and practice," *IEEE Trans. Fuzzy Syst.*, vol. 28, no. 9, pp. 1940–1950, Sep. 2020.

[31] A. Taghieh, A. Mohammadzadeh, C. Zhang, N. Kausar, and O. Castillo, "A type-3 fuzzy control for current sharing and voltage balancing in microgrids," *Appl. Soft Comput.*, vol. 129, Nov. 2022, Art. no. 109636. [Online]. Available: https://www.sciencedirect.com/science/article/pii/S1568494622006858

[32] A. Taghieh, C. Zhang, K. A. Alattas, Y. Bouteraa, S. Rathinasamy, and A. Mohammadzadeh, "A predictive type-3 fuzzy control for underactuated surface vehicles," *Ocean Eng.*, vol. 266, Dec. 2022, Art. no. 113014. [Online]. Available: https://www.sciencedirect.com/science/article/pii/S0029801822022971

[33] O. Elhaki, K. Shojaei, and A. Mohammadzadeh, "Robust state and output feedback prescribed performance interval type-3 fuzzy reinforcement learning controller for an unmanned aerial vehicle with actuator saturation," *IET Control Theory Appl.*, vol. 17, no. 5, pp. 605–627, Mar. 2023. [Online]. Available: https://ietresearch.onlinelibrary.wiley.com/doi/abs/10.1049/cth2.12415

[34] A. Mohammadzadeh and E. Kayacan, "A non-singleton type-2 fuzzy neural network with adaptive secondary membership for high dimensional applications," *Neurocomputing*, vol. 338, pp. 63–71, Apr. 2019.